Developing a coarse-grained force field for the diblock copolymer poly(styrene-b-butadiene) from atomistic simulation

Xuejin Li, Dazhi Kou, Shuling Rao, and Haojun Liang^{a)}
Hefei National Laboratory for Physical Sciences at Microscale, University of Science and Technology of China, Hefei, Anhui 230026, People's Republic of China and Department of Polymer Science and Engineering, University of Science and Technology of China, Hefei, Anhui 230026, People's Republic of China

(Received 16 February 2006; accepted 6 April 2006; published online 24 May 2006)

We have developed a coarse-grained force field for the poly(styrene-b-butadiene) diblock copolymer. We describe the computational methods and discuss how they were applied to develop a coarse-grained force field for this diblock copolymer from the atomistic simulation. The new force field contains three different bonds, four angles, five dihedral angles, and three nonbonded terms. We successfully tested this coarse-grained model against the chain properties, including static and dynamic properties, derived from the atomistic simulation; the results suggest that the coarse-grained force field is an effective model. © 2006 American Institute of Physics.

[DOI: 10.1063/1.2200694]

I. INTRODUCTION

With increasing computer power, computer simulation methods have become main pillars of scientific research and we are arriving quickly to a point where the simulation of complex systems, such as polymers, will become realizable. Presently, however, the quantitative modeling of polymer chains in full atomistic detail at meso- or macroscopic length scales remains difficult because of the huge number of degrees of freedom in such system. A possible solution to this problem is to reduce the number of degrees of freedom through the mapping of an atomistic model onto coarsegrained structures. In fact, some simple models for the study of meso- and macroscale phenomena in polymer systems have been used extensively, 1,2 but most of them do not distinguish between chemically different polymers because of their generic nature.

This paper describes a method for systematically generating coarse-grained (CG) models from atomistic models. In recent years, a number of so-called CG models have been developed to enhance polymer simulations, including bond fluctuation^{3–10} and high-coordination lattice^{11–13} models. Here we briefly describe a few of the major achievements: Clancy defined a long-range interaction energy and estimated a continuous effective potential energy between beads;¹⁴ Guerrault et al. built a mean force potential and used it to containing system polyethylene cis-polybutadiene; 15 Buchete et al. obtained anisotropic potentials for protein simulations that were extracted from the continually growing databases of protein structures; ¹⁶ Murat and Kremer mapped bead-spring-type polymer chains in a melt to a soft-core liquid with fluctuating ellipsoidal particles modeled by an anisotropic Gaussian potential; ¹⁷ Bolhuis et al. 18 and Louis 19 described a similar method for coarsening

polymer chains in dilute-to-semidilute solutions; and Tschöp et al. 20,21 and Hahn et al. 22 and Akkermans and Briels 23 performed systematic studies into polymer melt coarse graining and developed a hierarchy of methods to bridge the gap from microscopic to mesoscopic simulation. Of all the models that have been developed, the one that is closest to ours is a method devised by Müller-Plathe and co-workers to automatically adjust force fields for specific systems exhibiting mesoscale phenomena to polymeric systems.²⁴⁻²⁷ The main feature of these kinds of methods is the coarsening of the models and then using them to describe and reproduce many of the parameters of polymer properties obtained from atomistic simulations. When mapping atomistic structures onto coarse-grained models, a cluster of several atoms is usually considered as a single bead. The interaction energies between two beads are obtained through an optimization procedure that reproduces the structural distributions between the beads, which are obtained from atomistic simulations.

When developing simulation methods for polymers, we must consider the complex nature of these systems; for example, obtaining a meaningful coarse-grained force field for more-complex polymers, such as diblock copolymers, remains a great challenge. Diblock copolymers, which comprise two linear sequences of chemically different species (A and B), represent an interesting class of polymeric materials that exhibit a rich variety of phase behaviors, ²⁸ making them subjects of great interest for experiments, ^{29–33} theory, ^{34–38} and computer simulation. ^{39–42} The initial test of the approach by Muller-Plathe and co-workers used homopolymers as models.^{24–27} In this paper, we extend the coarse-graining strategy described above to block copolymers—specifically, to a symmetric diblock copolymer comprising A and B units of equal length. The introduction of the joint point among the blocks causes the problem to become slightly different and more complicated. We have to distinguish between unlike monomers when calculating the bond lengths, bond angles, dihedral angles, and radial distribution functions (RDFs). In-

a) Author to whom correspondence should be addressed. Electronic mail: hjliang@ustc.edu.cn

FIG. 1. Illustration of the mapping of poly(styrene-b-butadiene) from the atomistic to the mesoscopic level.

terference between these quantities causes the coarse-grained procedure to become difficult. As a first trial, a single symmetric diblock copolymer chain in vacuum as a model is performed in the simulation. When the method has been found to show promise, it can easily be extended to the case of multiple chains in the melt or in solution.

II. METHODS

A. Concept

Atomistic force fields of polymers are usually divided into two major parts, i.e., bonded and nonbonded potential terms, ²⁴ each of which comprises several different contributors. The total force field energy can be described as follows:

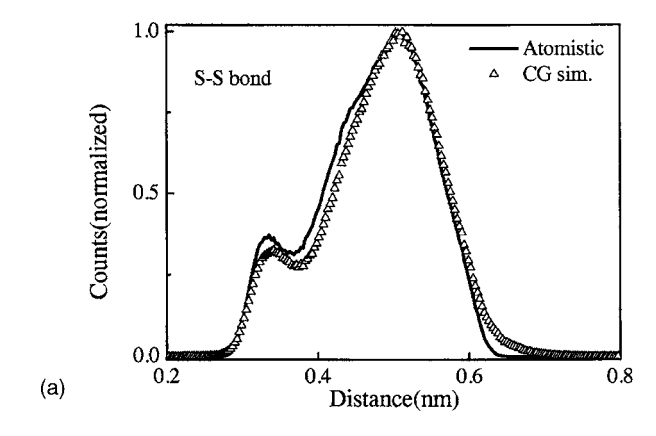
$$V_{\text{tot}} = V_{\text{bonded}} + V_{\text{nonbonded}} = (V_{\text{str}} + V_{\text{bend}} + V_{\text{tors}}) + (V_{\text{vdw}} + V_{\text{es}} + \cdots), \tag{1}$$

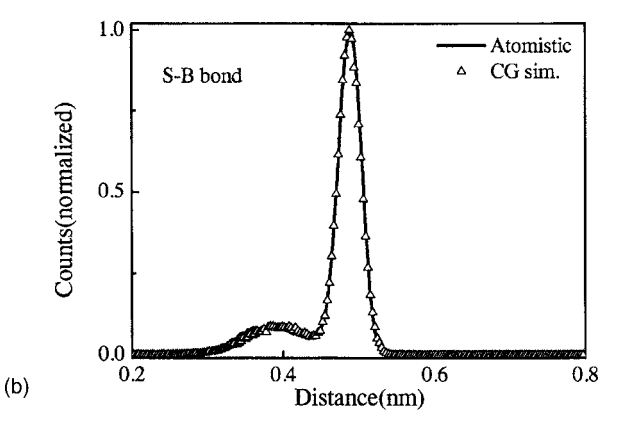
where V_{tot} is the total energy of the system; V_{str} and V_{bend} are the potentials defining the contributions for bond stretching between pairs of bonded atoms and the angular bending between three atoms, respectively; $V_{\rm tors}$ is a torsional potential accounting for the change of the energy as bonds rotate; $V_{\rm vdw}$ accounts for the excluded volume repulsive and intermolecular attractive forces between atoms in different polymer chains or in the same polymer chains, but at least three bonds apart; $V_{\rm es}$ is the potential of the electrostatic interactions.⁴³ The coarse-grained force field is constructed similarly using four potential terms, i.e., $V_{\rm str},~V_{\rm bend},~V_{\rm tors},$ and $V_{\rm nonbonded};$ we did not intend to make adjustments to all of the terms simultaneously but to perform successive adjustment of the terms in the order of their relative strength. According to the results described by Reith et al.,24 we chose to begin with the stretching energy and work our way systematically down to the torsional energy in the following order:

$$V_{\text{str}} \to V_{\text{bend}} \to V_{\text{nonbonded}} \to V_{\text{tors}}.$$
 (2)

B. Simulation

This paper describes the computational methods and their application to the development of a coarse-grained force field for the poly(styrene-b-butadiene) (PS-b-PB) diblock copolymer from the atomistic simulation. Thus, we had to construct a CG model of the PS-b-PB diblock copolymer. We choose this copolymer because of its wide applicability in industry, e.g., poly(styrene-co-butadiene) rubber





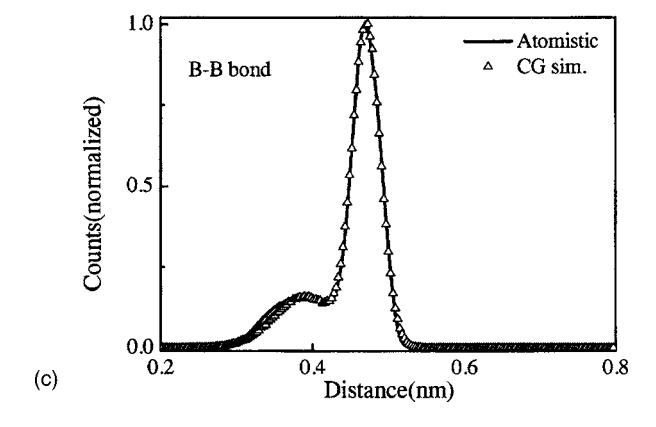


FIG. 2. Histograms of the (a) S–S, (b) S–B, and (c) B–B bond distributions of poly(styrene-*b*-butadiene) obtained through atomistic (solid lines) and coarse-grained (empty triangles) simulations at 500 K.

(SBR) is used in systems that are exposed to low temperatures. Our molecular dynamics simulations of this diblock copolymer, which comprises two species—styrene (S) and butadiene (B)—of equal length (ten monomers), in vacuum were performed using the program TINKER (Refs. 44–49) in an orthorhombic cubic box having standard periodic boundary conditions. The parameters of the all-atom force field for the polymer were obtained directly from the MM2 (Refs. 50–52) force field, and the CG force field was developed using our own new force field, which we designed to match the structural properties, such as radial distribution functions, of the various kinds of polymers derived from atomistic simulations.

The molecular dynamics were simulated using the Langevin equation of motion at a constant temperature T:

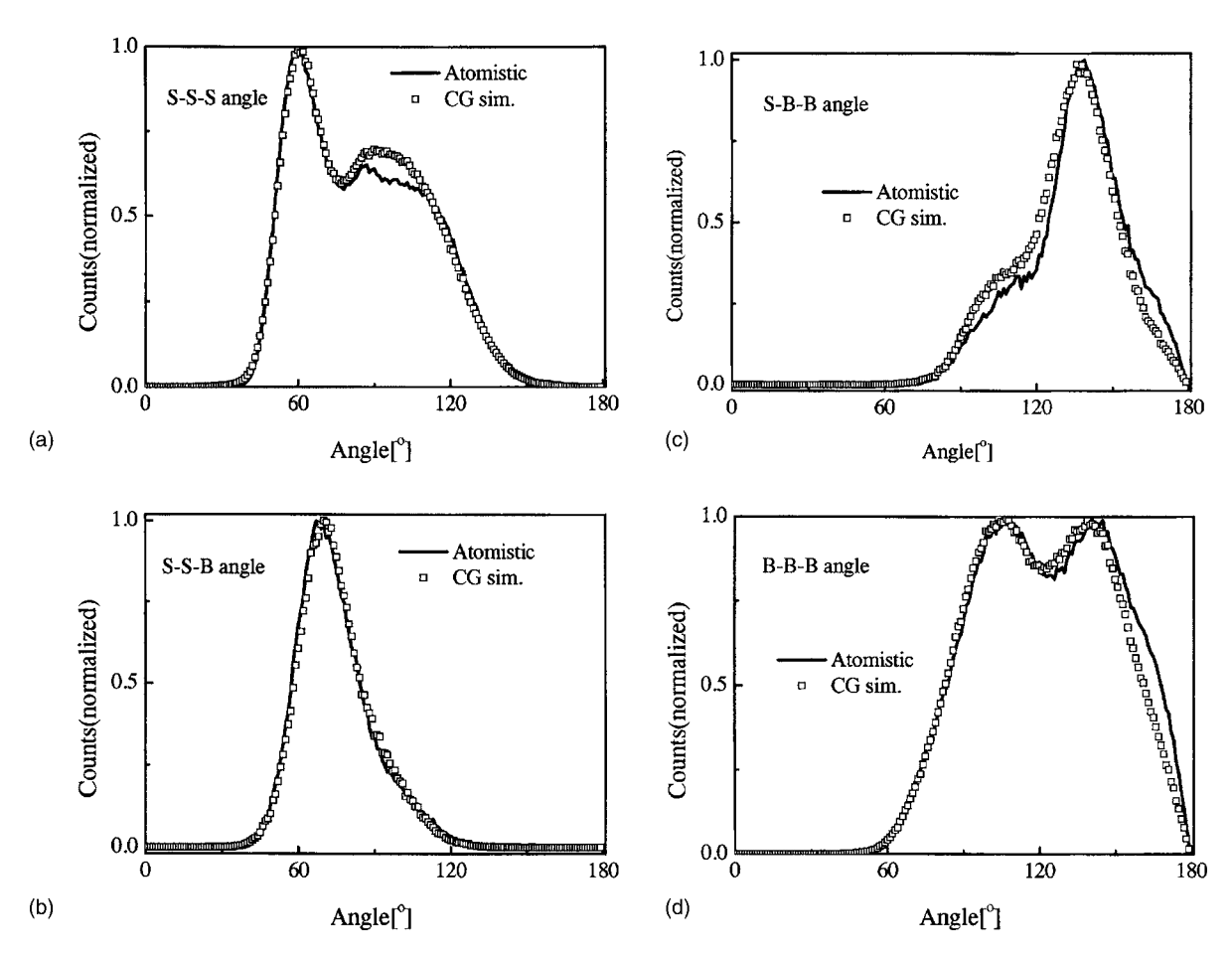


FIG. 3. Histograms of the (a) S–S–S, (b) S–S–B, (c) S–B–B, and (d) B–B–B angular distributions of poly(styrene-b-butadiene) obtained through atomistic (solid lines) and coarse-grained (empty squares) simulations at 500 K.

$$m_i \frac{d^2 \mathbf{r}_i}{dt^2} = -m_i \zeta_i \frac{d\mathbf{r}_i}{dt} + \sum_i F_{ij} + \xi_i,$$
 (3)

where \mathbf{r}_i is the position of the *i*th bead and $\Sigma_j \mathbf{F}_{ij}$ and ξ_i are the systematic and random forces, respectively, on the *i*th bead. The white and Gaussian random force ξ_i satisfy $\langle \xi_i \rangle = 0$ and its variance is $\langle \xi_i(t)\xi_j(t) \rangle = 2\zeta_i k_B T \delta_{ij} \delta_i \mathbf{I}$, where the bracket denotes the ensemble average and \mathbf{I} is a 3×3 unit matrix. The term ζ_i represents the friction coefficient of the *i*th bead; we used $\zeta_i = 0.91$ in the simulations. For numerical integration of the Langevin equation, we used the Velocity Verlet algorithm^{53,54} with a finite time step of 2 fs. The runs were performed in the *NVT* ensemble and the temperature was set at 500 K using an Andersen thermostat with the collision frequency v = 0.10.

To construct the coarse-grained models, we began from atomistic simulations from which we could obtain the distributions of bond lengths, bond angles, dihedral angles, and RDFs. The initial configurations were generated using the given parameters for the bonds, angles, dihedral angles, and other interactions according to the MM2 force field. The energy of the system was optimized to relax overlapping monomers, in which case the excluded volume problems were avoidable. Subsequently, the chain was placed randomly into the simulation box having periodic boundary conditions.

A preequilibration procedure was run initially at a higher temperature. The equilibration runs were performed until the distributions of bonds, angles, dihedral angles, and RDFs had stabilized. Subsequently, a run of more than 10⁶ integration steps was required to obtain smooth RDFs.

III. COARSE GRAINED FORCE FIELD DEVELOPMENT A. Mapping

The first step of the coarse-graining procedure was to choose the centers of the coarse-grained beads. Figure 1 illustrates the mapping of the S and B strands. Every S strand was replaced by one bead, centered at the mass center of the unit. In view of the particular features of the B strand, we applied a different type of bead in this case, i.e., we chose the center of the double bond of the unit to be the mapping point; a detailed description of the process is available elsewhere. ⁵⁶

The force field corresponding to this choice of coarse-grained model will have two types of coarse-grained beads (corresponding to the S and B strands), three different types of bonds (corresponding to three bond distributions: S–S, S–B, and B–B), and four types of angles (corresponding to four angle distributions: S–S–S, S–S–B, S–B–B, and B–B–B). By analogy, there should be five dihedral angle distributions (S–S–S–S, S–S–S–B, S–S–B–B, S–B–B, and B–B–B–B) and three RDFs (SS, SB, and BB).

B. Bonded potential

Figures 2(a)–2(c) display the distributions of distances between two successive coarse-grained beads along the chain, namely, the three bond distributions, SS, SB, and BB, respectively. The Bolzmann-inverted distribution was applied to obtain the bond energy in the CG simulations, as stated in Eq. (4).

$$V_{\text{str},i}(r) = -k_B T \ln(p_i(r)) \quad (i = SS, SB, BB). \tag{4}$$

Boltzmann inversion is a method that can always perform potential inversion from a distribution to yield a potential of mean force. Details on the Boltzmann-inversion method that we used are available elsewhere. Although the Boltzmann-inverted distribution provides only an approximation of the bond energy, it turns out that the CG simulations yield almost the same distributions; hence, no further optimizations were necessary.

For angles, we weighted the distributions of three successive beads along the chain by a factor of $\sin \alpha$ and then we used the Boltzmann-inverted angular distributions to obtain the angular potentials in the CG simulations, which are similar to the bond distributions.

$$V_{\text{bend}}(\alpha) = -k_B T \ln \left(\frac{p(\alpha)}{\sin \alpha} \right). \tag{5}$$

Figure 3 displays the results. The atomistic data (solid lines) are mapped well by the coarse-grained model (squares). Indeed, it was sufficiently reproduced such that further optimization was unnecessary.

For the distributions of the dihedral angles, we used a nonlinear curve fitting method to obtain the coarse-grained simulations' analytical potential function of dihedral angles. For the analytical potential, it is relatively straightforward to automatically adjust the parameters. We used a function having the Fourier progression form

$$V_{\text{dihedral}}(\theta) = \sum_{i=1}^{n} \frac{V_i}{2} (1 + \cos(i\theta - \gamma_i)). \tag{6}$$

Here, the values of the series γ_i $(i=1,2,\ldots,n)$ are constants. Compared to the distributions of the dihedral angles obtained from atomistic simulations, we adjusted the values of V_n (n=1-6) according to the distribution of the dihedral angles from the coarse-grained simulation. Table I lists the values of the parameters, and Fig. 4 displays their optimized distributions. We observe that the atomistic data (solid lines) are symmetrized and five-point smoothed. The coarse-grained data (circles) were obtained for the force field with torsional potentials; qualitatively, they reproduce the atomistic curve.

C. Nonbonded potential optimization

For the nonbonded portion of the potential, we illustrate the procedure using, as an example, the derivation of an effective nonbonded potential from a given target radial distribution function g(r). Assume that we begin with a tabulated initial potential $V_0(r)$. It has been proposed state that the inversion of the RDFs for one-component simple liquid systems may be performed through simple Boltzmann inversion of

TABLE I. Parameters of the dihedral angle potentials obtained through coarse-grained simulations of poly(styrene-b-butadiene) using Eq. (6).

Dihedral angle	n	i	V_{i}	γ_i (deg)
S–S–S	4	1	0.997	0
		2	0.536	180
		3	1.155	0
		4	0.948	0
S–S–S–B	5	1	16.612	0
		2	-7.199	180
		3	4.857	0
		4	1.004	0
		5	-1.342	0
S–S–B–B	6	1	2.827	0
		2	-4.467	180
		3	2.811	0
		4	-0.014	0
		5	0.234	0
		6	0.065	0
S-B-B-B	4	1	-4.507	0
		2	-1.222	180
		3	-0.170	0
		4	0.159	0
B-B-B-B	6	1	-3.261	0
		2	0.162	180
		3	0.591	0
		4	-0.034	0
		5	-0.027	0
		6	-0.080	0

g(r). This approach is exact, however, only at the limit of infinitely dilute systems. We use the potential of mean force,

$$F(r) = -k_B T \ln g(r), \tag{7}$$

which is a free energy and not a potential energy (except for the case of zero density). However, F(r) is usually sufficient to serve as the initial guess $V_0(r)$ in an iterative procedure. The potential must be improved using a correction term. This step can be iterated as follows:

$$V_{i+1}(r) = V_i(r) + k_B T \ln \frac{g_i(r)}{g(r)}$$
 (8)

until

$$f_{\text{target}} = \int \omega(r)(g(r) - g_j(r))^2 dr$$
 (9)

measures the curve convergence quantitatively. As a weighting function, we applied the expression $\omega(r) = \exp(-r)$ to cause stronger deviations at small distances.

Figure 5 indicates that a reasonably good relationship exists between the RDFs obtained from the atomistic and CG simulations. The RDFs obtained from the CG simulations reproduce both the rises of the main peaks and their convergences. The coarse-grained RDFs agree well to the RDFs

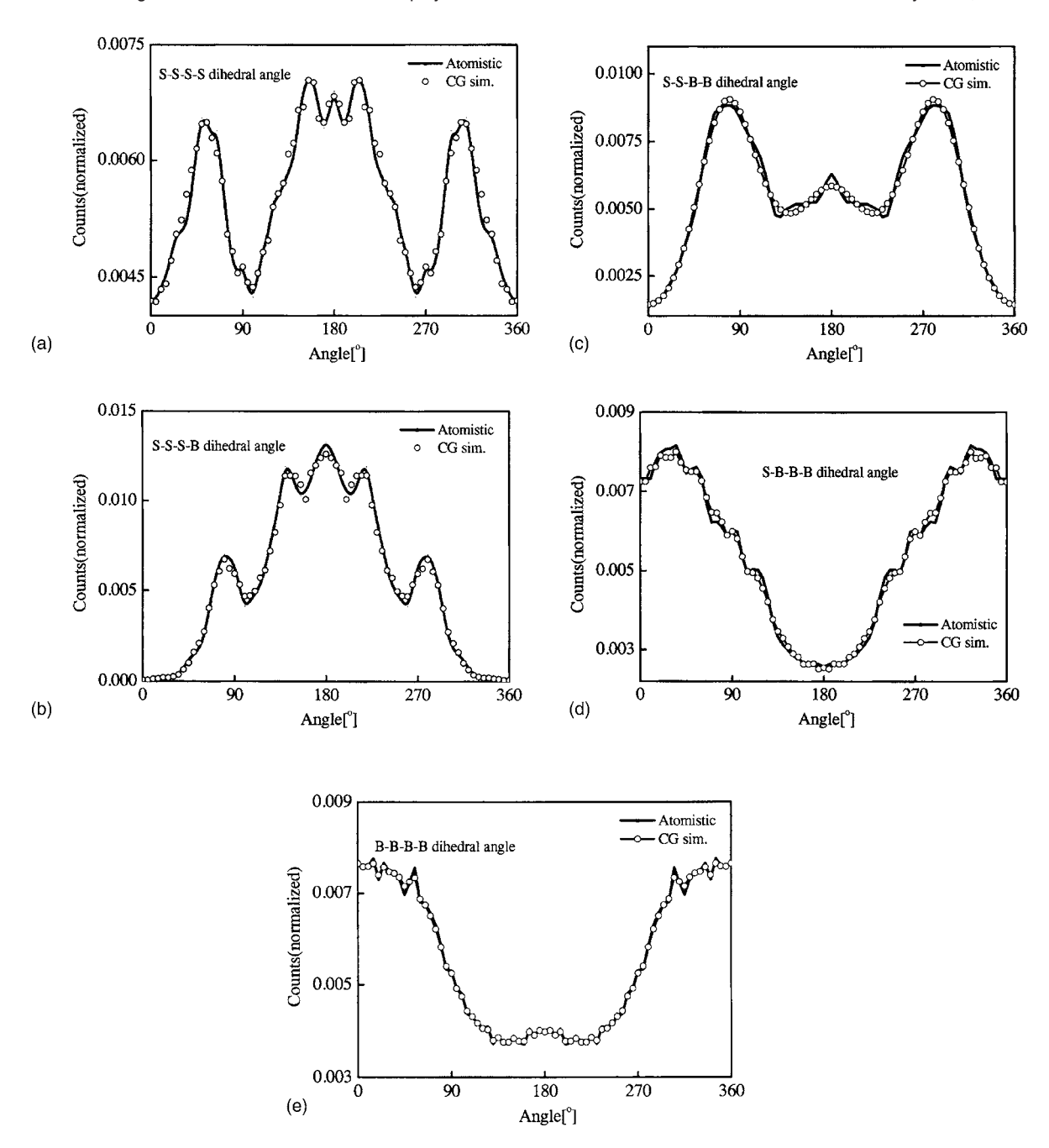


FIG. 4. Normalized distributions of the (a) S–S–S–S, (b) S–S–S–B, (c) S–S–B–B, (d) S–B–B–B, and (e) B–B–B–B dihedral angles of poly(styrene-b-butadiene) obtained through atomistic (solid lines) and coarse-grained (empty circles) simulations at 500 K.

obtained from the atomistic simulations. Figure 6 displays the corrected numerical potentials of the coarse-grained simulation that correspond to those in atomistic simulations.

IV. STATIC AND DYNAMIC PROPERTIES OF DIBLOCK COPOLYMERS

In this section, we discuss some of the polymer chain properties, both static and dynamic, determined through atomistic and coarse-grained simulations to demonstrate that our coarse-grained model does indeed reproduce the results from the atomistic simulations.

Table II lists the statistical values of the mean-square end-to-end distance $(\langle R_G^2 \rangle)$ and the mean-square radius of

gyration $(\langle S_G^2 \rangle)$ obtained. The coarse-grained force field reproduced the properties of the atomistic model.

Of more interest is the finding that the diffusion of the coarse-grained molecular dynamics simulation for PS-b-PB displays the same characteristics as that obtained from an atomistic molecular dynamics simulation. The diffusion co-

TABLE II. Mean-square end-to-end distances and mean-square radii of gyration obtained through atomistic and coarse-grained simulations of poly(styrene-b-butadiene).

Simulation	$\langle R_G^2 \rangle / \text{nm}^2$	$\langle S_G^2 \rangle / \text{nm}^2$	$\langle R_G^2 \rangle / \langle S_G^2 \rangle$
Atomistic	3.1162	0.6055	5.1465
CG	3.1321	0.6029	5.1951

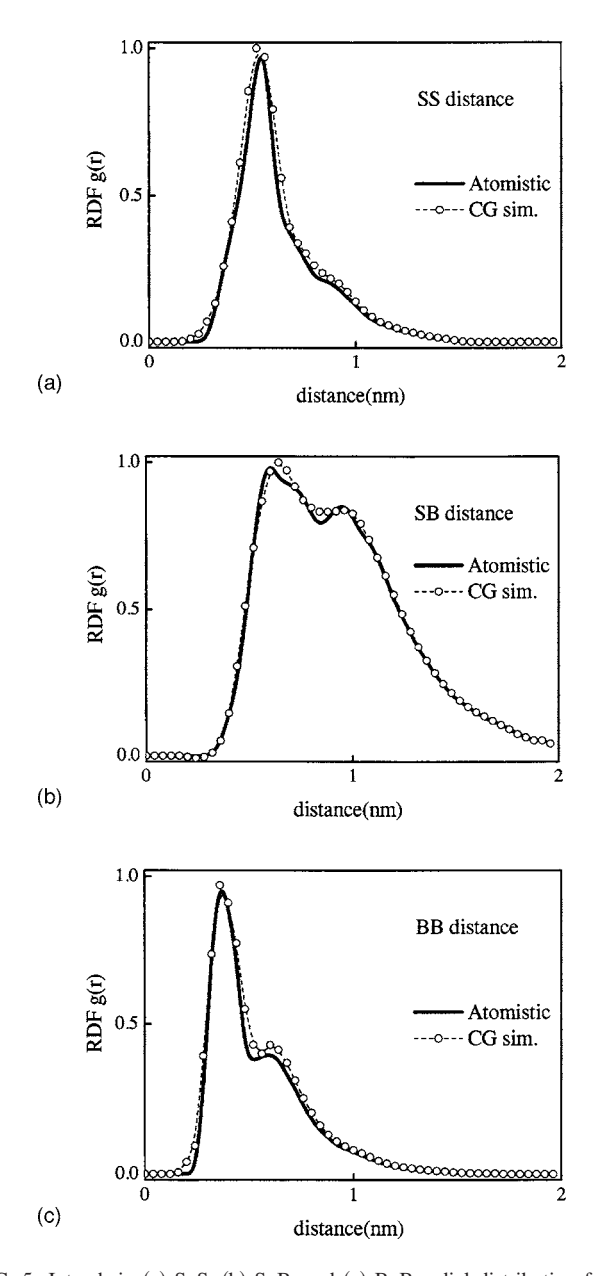


FIG. 5. Intrachain (a) S-S, (b) S-B, and (c) B-B radial distribution functions (RDFs) of poly(styrene-b-butadiene) obtained through atomistic (solid lines) and coarse-grained (empty squares, broken lines) simulations at 500 K. The latter approach reproduces both the rise of the main peaks and the convergence.

efficient was measured by monitoring the mean-square displacement (MSD) of the center of gravity of the chains, ^{59,60}

$$D = \frac{1}{6} \lim \frac{g_{\text{CG}}(t)}{t} = \frac{1}{6} \lim \frac{\partial}{\partial t} \langle (r_i(t) - r_i(0))^2 \rangle, \tag{10}$$

where the quantity in braces is the ensemble-averaged meansquare displacement of the molecules and $r_i(t)$ is the vector coordinate of the center of mass of bead i. Figure 7 displays the mean-square displacements of the atomistic and coarsegrained simulations at 500 K and 101.3 kPa. The results from the simulations are shifted in log t to bring both sets of curves into coincidence. As expressed in the form of plots of the MSDs versus time, we do indeed observe a linear dependence of the MSDs with respect to t; the MSDs are linear up to 80 ns with this regime (slope: 0.49), followed by another

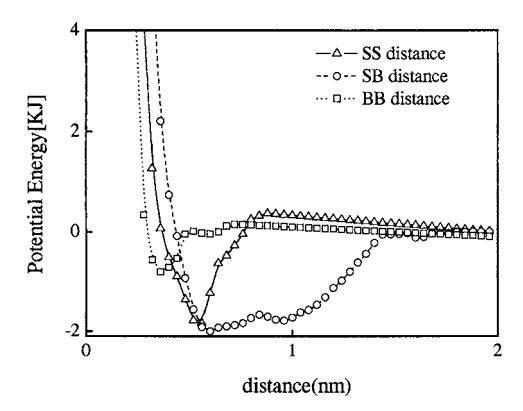


FIG. 6. Optimized nonbonded numerical potentials obtained through coarsegrained simulations of (a) S-S, (b) S-B, and (c) B-B interactions.

linear regime having a slope of 0.92. There are a few examples of the dynamic properties of coarse-grained simulations agreeing with experimental values and/or the atomistic simulations being observed in other simulations. ^{20,25,56,61} Our findings provide another example where, through multiscaling, a calculated dynamic property reproduced the results of atomistic simulations.

V. CONCLUSIONS

This paper describes the results of a molecular dynamics simulations of the diblock copolymer PS-b-PB. We developed an all-atom force field for this diblock copolymer using the MM2 force field and then developed coarse-grained models using this new force field. We designed these CG models to match the structural properties—such as RDFs of various kinds—that are derived through the use of atomistic simulations. Although we developed CG force fields only for PS-b-PB, this approach should be amenable for use with other diblock copolymer systems and, indeed, other polymer systems in general.

The optimization algorithm we used was quite powerful, but in one case—i.e., for the distribution of the dihedral angle—although the CG simulation's data reproduced the atomistic curve, the efficiency of this simulation was poor. We had hoped to obtain an effective potential for this term

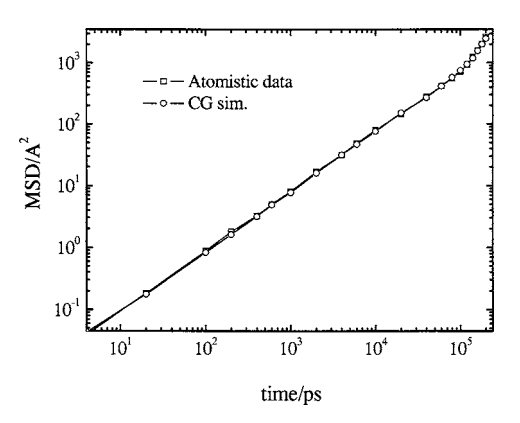


FIG. 7. The mean-square displacements of the center mass as a function of time for the poly(styrene-b-butadiene) chain at 500 K and 101.3 kPa obtained through atomistic molecular dynamics (empty circles, solid line) and coarse-grained molecular dynamics (empty squares, solid line) simulations, after shifting in $\log t$ to bring both sets of curves into coincidence.

through iterative methods, but it did not appear to converge slowly through these methods; our results proved this approach to be ineffectual. We used a nonlinear curve fitting method to obtain the coarse-grained simulations' analytical potential function for dihedral angles. For the analytical potential, it is relatively straightforward to adjust the parameters. Compared to the distributions of the dihedral angles obtained from atomistic simulations, we need to adjust the values of V_n (n=1-6) according to the distribution of the dihedral angles from the coarse-grained simulation. Hence, to some extent, the generated potential caused the program execution to be slow. Our analysis of the static and dynamic characteristics determined using the atomistic and coarse-grained simulations indicated that the latter approach provided accurate results.

ACKNOWLEDGMENTS

We are grateful for the financial support provided by the Outstanding Youth Fund (No. 20525416), the Programs of the National Natural Science Foundation of China (Nos. 20490220, 20374050, and 90403022), the National Basic Research Program of China (No. 2005CB623800), and KJCX2-SW-H14.

- ¹P. G. de Gennes, *Scaling Concepts in Polymer Physics* (Cornell University Press, Ithaca, 1979).
- ²M. Doi and S. F. Edwards, *The Theory of Polymer Dynamics* (Oxford University Press, Oxford, 1986).
- ³I. Carmesin and K. Kremer, Macromolecules **21**, 2819 (1988).
- ⁴W. Paul, K. Binder, K. Kremer, and D. W. Heermann, Macromolecules 24, 6332 (1991).
- ⁵H. P. Deutsch and K. Binder, J. Chem. Phys. **94**, 2294 (1991).
- ⁶J. Baschnagel, K. Binder, W. Paul, M. Laso, U. W. Suter, I. Batoulis, W. Jilge, and T. Bürger, J. Chem. Phys. **95**, 6014 (1991).
- ⁷ W. Paul, K. Binder, D. W. Heermann, and K. Kremer, J. Chem. Phys. **95**, 7726 (1991).
- ⁸W. Paul, K. Binder, D. W. Heermann, and K. Kremer, J. Phys. II 1, 37 (1991).
- ⁹H. P. Wittmann, K. Kremer, and K. Binder, J. Chem. Phys. **96**, 6291 (1992)
- ¹⁰ J. Baschnagel, W. Paul, V. Tries, and K. Binder, Macromolecules 31, 3856 (1998).
- ¹¹ J. Cho and W. L. Mattice, Macromolecules **30**, 637 (1997).
- ¹²T. Haliloglu and W. L. Mattice, J. Chem. Phys. **108**, 6989 (1998).
- ¹³ R. F. Rapold and W. L. Mattice, J. Chem. Soc., Faraday Trans. **91**, 2435 (1995).
- ¹⁴T. C. Clancy, Polymer **45**, 7001 (2004).
- ¹⁵ X. Guerrault, B. Rousseau, and J. Farago, J. Chem. Phys. **121**, 6538 (2004).
- ¹⁶N. V. Buchete, J. E. Straub, and D. Thirumalai, Polymer **45**, 597 (2004).
- ¹⁷M. Murat and K. Kremer, J. Chem. Phys. **108**, 4340 (1998).
- ¹⁸ P. G. Bolhuis, A. A. Louis, J. P. Hansen, and E. J. Meijer, J. Chem. Phys. 114, 4296 (2001).
- ¹⁹ A. A. Louis, Philos. Trans. R. Soc. London, Ser. A 359, 939 (2001).

- ²⁰ W. Tschöp, K. Kremer, J. Batoulis, T. Bürger, and O. Hahn, Acta Polym. 49, 61 (1998).
- ²¹ W. Tschöp, K. Kremer, O. Hahn, J. Batoulis, and T. Bürger, Acta Polym. 49, 75 (1998).
- ²²O. Hahn, L. Delle Site, and K. Kremer, Macromol. Theory Simul. 10, 288 (2001).
- ²³R. L. C. Akkermans and W. J. Briels, J. Chem. Phys. **114**, 1020 (2001).
- ²⁴D. Reith, H. Meyer, and F. Müller-Plathe, Macromolecules 34, 2335 (2001)
- ²⁵ D. Reith, H. Meyer, and F. Müller-Plathe, Comput. Phys. Commun. 148, 299 (2002).
- ²⁶ D. Reith, M. Pütz, and F. Müller-Plathe, J. Comput. Chem. **24**, 1624 (2003).
- ²⁷G. Milano and F. Müller-Plathe, J. Phys. Chem. B **109**, 18609 (2005).
- ²⁸ F. S. Bates and G. H. Fredrickson, Annu. Rev. Phys. Chem. 41, 525 (1990)
- ²⁹ T. Hashimoto, H. Tanaka, and H. Hasegawa, Macromolecules 18, 1864 (1985).
- ³⁰ F. S. Bates, J. H. Rosedale, G. H. Fredrickson, and C. J. Glinka, Phys. Rev. Lett. **61**, 2229 (1988).
- ³¹ J. H. Rosedale and F. S. Bates, Macromolecules **23**, 2329 (1990).
- ³² S. H. Anastasiadis, T. P. Russell, S. K. Satija, and C. F. Majkrzak, J. Chem. Phys. **92**, 5677 (1990).
- ³³ A. Menelle, T. P. Russell, S. H. Anastasiadis, S. K. Satija, and C. F. Majkrzak, Phys. Rev. Lett. **68**, 67 (1992).
- ³⁴L. Leibler, Macromolecules **13**, 1602 (1980).
- ³⁵ J. L. Barrat and G. H. Fredrickson, J. Chem. Phys. **95**, 1281 (1991).
- ³⁶ A. N. Semenov, Zh. Eksp. Teor. Fiz. **88**, 1242 (1985).
- ³⁷M. Olvera de la Cruz, Phys. Rev. Lett. **67**, 85 (1991).
- ³⁸ H. Benoit and G. Hadziioannou, Macromolecules **21**, 1449 (1988).
- ³⁹ H. Fried and K. Binder, J. Chem. Phys. **94**, 8349 (1991).
- ⁴⁰K. Binder and H. Fried, Macromolecules **26**, 6878 (1993).
- ⁴¹ A. Weyersberg and T. A. Vilgis, Phys. Rev. E **48**, 377 (1993).
- ⁴²R. G. Larson, Macromolecules **27**, 4198 (1994).
- ⁴³ A. R. Leach, *Molecular Modeling: Principles and Applications*, 2nd ed. (Prentice Hall, New Jersey, 2001).
- ⁴⁴ J. W. Ponde and F. M. Richards, J. Comput. Chem. **8**, 1016 (1987).
- ⁴⁵C. E. Kundrot, J. W. Ponder, and F. M. Richards, J. Comput. Chem. **12**, 402 (1991).
- ⁴⁶ M. E. Hodsdon, J. W. Ponder, and D. P. Cistola, J. Mol. Biol. **264**, 585 (1996).
- ⁴⁷ R. V. Pappu, R. K. Hart, and J. W. Ponder, J. Phys. Chem. B **102**, 9725 (1998).
- ⁴⁸P. Ren and J. W. Ponder, J. Comput. Chem. **23**, 1497 (2002).
- ⁴⁹P. Ren and J. W. Ponder, J. Phys. Chem. B **107**, 5933 (2003).
- ⁵⁰N. L. Allinger, J. Am. Chem. Soc. **99**, 8127 (1977).
- ⁵¹ J. T. Sprague, J. C. Tai, Y. Yuh, and N. L. Allinger, J. Comput. Chem. 8, 581 (1987).
- ⁵² N. L. Allinger, R. A. Kok, and M. R. Imam, J. Comput. Chem. 9, 591 (1988).
- ⁵³M. P. Allen, Mol. Phys. **40**, 1073 (1980).
- ⁵⁴F. Guarnieri and W. C. Still, J. Comput. Chem. **15**, 1302 (1994).
- ⁵⁵ H. C. Andersen, J. Chem. Phys. **72**, 2384 (1980).
- ⁵⁶ X. J. Li, X. J. Ma, L. Huang, and H. J. Liang, Polymer **46**, 6507 (2005).
- ⁵⁷F. Müller-Plathe, ChemPhysChem **3**, 754 (2002).
- ⁵⁸ A. K. Soper, Chem. Phys. **202**, 295 (1996).
- ⁵⁹ J. Baschnagel, K. Binder, P. Doruker *et al.*, Adv. Polym. Sci. **152**, 41 (2000).
- ⁶⁰T. I. Morrow and E. J. Maginn, J. Phys. Chem. B **106**, 12807 (2002).
- ⁶¹ K. R. Haire, T. J. Carver, and A. H. Windle, Comput. Theor. Polym. Sci. 11, 17 (2001).